Bi-Level Optimal Design of Integrated Energy System With Synergy of Renewables, Conversion, Storage, and Demand

Lizhi Zhang, Hui Zhang, Fan Li, and Bo Sun, *Member, IEEE*

***Abstract*—Integrated energy systems (IESs) that combine biogas, solar, and wind energy sources demonstrate considerable potential for effective utilization of renewable energy, which is instrumental for achieving carbon neutrality. The enhancement in their energetic and economic performances relies on optimal design methods that need to consider the combined optimization of capacity and operation and synergy between biogas production, energy conversion, storage, and demand. Therefore, this study proposes a bi-level optimal design method for a biogas–solar–wind IES. First, an exergy hub model is established to accurately describe the variations in the energy quantity and quality resulting from energy conversion processes. Then, the combined capacity and operation optimization problem of the IES is formulated as a bi-level iterative model, and a full-time-series clustering method based on multi-attribute weighting is employed to obtain typical source–load scenarios. The first level is designed to maximize the cost and exergy savings and determine the rated capacities of renewables, energy conversion and storage components; the second level synergistically optimizes the operation schemes of energy conversion, storage, and demand components by incorporating a thermodynamic model of biogas production along with an electrical demand response program. And the iterative optimization mechanisms between these two levels are established. Moreover, a hybrid algorithm combining a genetic algorithm and sequential quadratic programming method is developed to solve the bi-level model. Finally, the feasibility and effectiveness of the proposed method are verified through case studies.**

***Index Terms*—Bi-level optimal design, demand response, exergy hub model, hybrid algorithm, integrated energy system.**

NOMENCLATURE

Abbreviations

AC	Absorption chiller.
ACSR	Annual cost saving ratio.
AD	Anaerobic digester.
AESR	Annual exergy saving ratio.
BPGU	Biogas-fired power generation unit.
DCSR	Daily cost saving ratio.
DESR	Daily exergy saving ratio.
DR	Demand response.
EC	Electric chiller.
EQC	Energy quality coefficient.
GA	Genetic algorithm.
GB	Gas boiler.
HS	Heat storage.
IES	Integrated energy system.
PV	Photovoltaic.
SP	Separate production.
SQP	Sequential quadratic programming.
WT	Wind turbine.

Indices and Sets

i	Index of components.
j	Index of time series data.
s	Index of source–load scenarios.
t	Index of time periods.
X_{first}	Set of optimization variables in the first level model.
X^s_{second}	Set of optimization variables in the second level model in s.
Ω	Set of components.

Parameters

B	Ultimate CH_4 yield.
$C_{\text{IES/SP}}$	Annual total cost of IES/SP.
$C_{\text{IES/SP,cap}}$	Initial capital cost of IES/SP.
$C_{\text{IES,ic}}$	Annualized investment cost of IES.
$C_{\text{IES,mc/oc}}$	Annual maintenance/operation cost of IES.
$C_{\text{SP,oc}}$	Annual operation cost of SP.
$C^s_{\text{IES,oc}}$	Operation cost of IES in s.
$C_{\text{IES,bf/ng/grid}}$	Annual cost of biomass feedstock/natural gas/interacting with grid for IES.
CE_{IES}	Annual carbon emission of IES.

Received 23 November 2023; revised 20 August 2024; accepted 6 November 2024. Date of publication 3 January 2025; date of current version 4 April 2025. Paper 2023-PSEC-1802.R1, presented at the 2022 4th International Conference on Smart Power & Internet Energy Systems, Beijing, China, Dec. 09-12, and approved for publication in the IEEE TRANSACTIONS ON INDUSTRY APPLICATIONS by the Power Systems Engineering Committee of the IEEE Industry Applications Society [DOI: 10.1109/SPIES55999.2022.10082090]. This work was supported by the National Natural Science Foundation of China under Grant 61821004, Grant 62192753, and Grant 62103239. *(Corresponding author: Bo Sun.)*

Lizhi Zhang is with the School of Control Science and Engineering, Shandong University, Jinan 250061, China, and also with the Shandong Police College, Jinan 250200, China (e-mail: zhanglizhi0518@163.com).

Hui Zhang, Fan Li, and Bo Sun are with the School of Control Science and Engineering, Shandong University, Jinan 250061, China (e-mail: 202234949@mail.sdu.edu.cn; lifan1212@sdu.edu.cn; sunbo@sdu.edu.cn).

Color versions of one or more figures in this article are available at https://doi.org/10.1109/TIA.2024.3524950.

Digital Object Identifier 10.1109/TIA.2024.3524950

CE^{s}_{IES}	Carbon emission of IES in *s*.
$D_{\mathrm{bio,max}}$	Maximum daily biogas yield.
D^{s}	Number of days for scenario *s*.
HRT	Hydraulic retention time.
$LHV_{\mathrm{ng/bio}}$	Lower heating value of natural gas/biogas.
$N_{i,\max}$	Maximum rated capacity of component *i*.
N_s	Number of source–load scenarios.
n_i	Lifespan of component *i*.
P_{ng}	Natural gas price.
P_{ct}	Unit price of the carbon tax.
$P^{s,t}_{\mathrm{grid}}$	Electricity price comprising the electricity purchase and sales prices in *s* at *t*.
Pb_{IES}	Payback period of IES.
R_i	Capital recovery factor of component *i*.
S	Influent total volatile solids concentration.
T_{AD}	Fermentation temperature of AD.
T_{a}	Ambient temperature.
$T_{\mathrm{ng/bio}}$	Complete combustion temperature of natural gas/biogas.
$T_{\mathrm{h/c}}$	Temperature of heat/cold water.
UIC_i	Unit investment cost of component *i*.
UMC_i	Unit maintenance cost of component *i*.
Δt	Time interval.
ω	Weighting of optimization objective.
$\lambda_{\mathrm{e/h/c}}$	Energy quality coefficient of electricity/heat water/cold water.
$\lambda_{\mathrm{ng/bio}}$	Energy quality coefficient of natural gas/biogas.
$\mu_{\mathrm{grid/ng/bio}}$	Emission conversion factor of grid/natural gas/biogas.
β	Proportion of translational load to the original electricity load.
$\eta^{\mathrm{rated}}_{\mathrm{BPGU,e}}$	Rated power generation efficiency of BPGU.
$\eta_{\mathrm{BPGU,e/h}}$	Electricity/heat efficiency of BPGU.
$\eta_{\mathrm{GB/HS}}$	Efficiency of GB/HS.

Variables

D_{bio}	Daily biogas yield.
$En_{\mathrm{load,e/h/c}}$	Electricity/heating/cooling load.
$En_{\mathrm{PV/WT/BPGU,e}}$	Electricity output of PV/WT/BPGU.
$En_{\mathrm{BPGU,bio}}$	Biogas consumption of BPGU.
$En_{\mathrm{BPGU,h}}$	Recovered heat from BPGU.
$En_{\mathrm{grid,e}}$	Electricity interacting with grid including purchasing/selling electricity.
$En_{\mathrm{AC/AD,h}}$	Heat consumption of AC/AD.
$En_{\mathrm{GB,h}}$	Heat output of GB.
$En_{\mathrm{HS,h}}$	Heat discharging or charging of HS.
$En_{\mathrm{EC/AC,c}}$	Cold output of EC/AC.
En^{s}_{ng}	Natural gas consumption of IES in *s*.
En^{s}_{bio}	Biogas consumption of IES in *s*.
$En^{s,t}_{\mathrm{grid,e}}$	Electricity interacting with grid including purchasing/selling electricity in *s* at *t*.
$En^{s,t}_{\mathrm{grid,e,+}}$	Purchased electricity from grid in *s* at *t*.
$En^{s,t}_{\mathrm{BPGU,e}}$	Electricity output of BPGU in *s* at *t*.
$En^{s,t}_{\mathrm{EC,c}}$	Cold output of EC in *s* at *t*.
$En^{s,t}_{\mathrm{HS,h}}$	Heat discharging or charging of HS in *s* at *t*.
$En^{s,t}_{\mathrm{HS,h,state}}$	Storage state of HS in *s* at *t*.
$Ex_{\mathrm{load,e/h/c}}$	Exergy of electricity/heating/cooling load.
$Ex_{\mathrm{PV/WT/BPGU,e}}$	Exergy of electricity output for PV/WT/BPGU.
$Ex_{\mathrm{grid,e}}$	Exergy of electricity interacting with grid including purchasing/selling electricity.
$Ex_{\mathrm{AD,h}}$	Exergy of heat consumption for AD.
$Ex_{\mathrm{GB,h}}$	Exergy of heat output for GB.
$Ex_{\mathrm{GB,ng,in}}$	Exergy of natural gas consumption for GB.
$Ex_{\mathrm{GB,bio,in}}$	Exergy of biogas consumption for GB.
$Ex_{\mathrm{HS,h}}$	Exergy of heat discharging or charging for HS.
$Ex_{\mathrm{EC/AC,c}}$	Exergy of cold output for EC/AC.
$Ex^{s,t}_{\mathrm{BPGU,e}}$	Exergy of electricity output for BPGU in *s* at *t*.
$Ex^{s,t}_{\mathrm{EC,c}}$	Exergy of cold output for EC in *s* at *t*.
$Ex^{s,t}_{\mathrm{grid,e,+}}$	Exergy of purchased electricity from grid in *s* at *t*.
$Ex^{s,t}_{\mathrm{HS,h}}$	Exergy of heat discharging or charging for HS in *s* at *t*.
$Ex^{s,t}_{\mathrm{HS,h,state}}$	Exergy of storage state for HS in *s* at *t*.
$Ex^{s,t}_{\mathrm{load,e,ori}}$	Exergy of original electricity load in *s* at *t*.
$Ex^{s,t}_{\mathrm{load,e,tran}}$	Exergy of translational electricity load in *s* at *t*.
$Ex^{s,t}_{\mathrm{re}}$	Exergy input of renewable energy in *s* at *t*.
$Ex^{s}_{\mathrm{in,IES}}$	Exergy input of IES in *s*.
$Ex_{\mathrm{in,IES/SP}}$	Annual exergy input of IES/SP.
$N_{\mathrm{BPGU/EC/HS}}$	Rated capacity of BPGU/EC/HS.

I. Introduction

DEPLETION of fossil energy reserves and environmental degradation have spurred global advocacy for the advancement of clean energy initiatives to achieve carbon neutrality [1]. To mitigate our reliance on fossil fuels and curtail the greenhouse effect, the proliferation of renewable energy sources is a pivotal strategy [2]. Among these, biogas emerges as a particularly promising candidate owing to its inexhaustibility and diverse sources [3], making it a suitable primary energy source for distributed IESs [4]. In rural locales, IESs based on biogas offer a robust mechanism to effectively furnish both electrical and thermal energy [5]. Unlike solar and wind energy, biogas is independent of meteorological conditions, which makes it a consistent and stable source of renewable energy that can ensure

an uninterrupted power supply [6]. This attribute renders biogas particularly suitable for combination with other renewable energies within IESs, thereby enhancing their capability to buffer the inherent intermittency of renewable sources [7].

Studies on IESs have examined several multi-energy complementary solutions. Gazda et al. [8] integrated a PV system to a biogas-fueled IES, and the experimental results indicated a reduction in the average relative energy consumption and carbon emissions by 54.50% and 67.37%, respectively, compared with a SP system. Wu et al. [9] developed a multi-objective operation optimization model of an IES based on biogas–solar–wind renewables and revealed that the proposed system had a more economical and ecofriendly operation effect than a natural gas–solar–wind IES. Zhou et al. [10] demonstrated that the synergistic utilization of biogas with solar energy can extend battery lifespans. System design emerges as a crucial technological facet of IESs [11], with direct implications for their operational efficiency, economic viability, and reliability [12]. Although the integration of biogas with diverse renewable energy sources confers advantages with respect to cost and energy conservation, it simultaneously increases the complexity and challenges associated with system design.

Various design approaches have been developed to determine the capacities of biogas-based IESs. Wang et al. [13] employed a nondominated GA to optimize the capacity of a biogas–solar IES, resulting in an energy-efficient and cost-effective performance. Sarkar et al. [14] constructed a hybrid microgrid comprising PV, WT, and biogas and used the HOMER simulation to optimize the capacities of various renewables for ensuring power supply stability. Su et al. [15] developed a heating load model for a biogas digester and optimized the capacity of a biogas–solar IES considering the heat consumption of biogas production. These studies primarily focused on optimizing system capacities without using advanced operation optimization technologies. However, system components often operate under off-design conditions due to the intermittency and fluctuation of renewable energy [16], making the capacity configuration and operation optimization of IESs become strongly coupled.

To address the aforementioned issue, multiple combined capacity and operation optimization methods have been proposed for renewable-based IESs. Fu et al. [17] proposed a coordinated capacity and operation optimization method for an IES considering the off-design characteristics of energy conversion components to minimize the annual total cost. Ji et al. [18] introduced a mixed-integer linear programming model to identify the optimal capacity and operation scheme for a solar–biomass hybrid system and evaluated the economic performance of the IES through the levelized cost of energy. Zhang et al. [19] developed a nested optimal planning method for a biogas–PV IES to simultaneously optimize the capacity and operation scheme, which improved the economic performance and renewable energy utilization of the system. Given the complexity of combined optimization, such methods typically use seasonal source–load data (transition season, summer, and winter) instead of full-year data, simplifying the problem. Li et al. [20] employed a modified uncertainty model to generate a range of operational scenarios and developed a two-stage mixed-integer linear programming model for the optimal design of a islanded solar–biogas IES, which was solved using the Benders Decomposition method. Theoretically, the daily production of biogas is a crucial design variable as it limits the capacities of energy conversion components and influences the distribution of thermal energy within IESs. Although the biogas application is considered in some IES optimal design methods, it tends to be defined as a given input rather than an optimization object, resulting in inaccurate design schemes and suboptimal performance. Furthermore, although DR has been demonstrated to facilitate energy balances under renewable intermittency [21], studies have focused only on the optimization of the energy supply side of IESs and ignored the load shifting of the demand side. However, the introduction of thermodynamic model-based biogas production optimization and DR leads to strong coupling and nonlinearity, considerably increasing the difficulty of solving combined optimization problems.

Regarding the selection of optimization objectives, several studies prioritize metrics such as energy consumption, cost, and carbon emissions [22]. For instance, the primary energy saving rate serves as the objective for optimization models in [13] and [19], while the goal is to minimize annual total costs in [20] and [23]. However, IESs are distinguished by their ability to integrate multiple forms of energy, such as natural gas, electricity, and thermal energy, and their key benefit lies in the cascade utilization of these energies, which offers a contrast to conventional single-energy systems [24]. The evaluation indices based on the first law of thermodynamics focus on the quantitative utilization of energy, overlooking the quality disparities among different energy types. Such indices fall short of providing an accurate assessment of energy use in biogas-based IESs.

To address these gaps identified in literatures, this study proposes a bi-level optimal design method for a biogas–solar–wind IES and performs case studies to verify the feasibility and effectiveness of the proposed method. The proposed method is scalable and can provide economical, efficient, and low-carbon design schemes for different mixes of energy supply technologies. The key contributions are summarized as follows:

- An exergy hub model is established for the biogas–solar–wind IES that describes the variations in energy quantity and quality during energy conversion, offering a more comprehensive assessment of energy utilization levels.
- The study incorporates a thermodynamic model for biogas production and an electrical DR program into the optimal design of the IES, creating a synergistic optimization of renewables, energy conversion, storage, and demand components.
- The combined capacity and operation optimization problem is formulated as a bi-level iterative optimization model, targeting cost and exergy savings. Moreover, a full-time-series clustering method based on multi-attribute weighting is developed to define typical source–load scenarios.

The structure of this study is as follows: Section II elucidates the structure and the exergy hub model of the IES. Section III describes the bi-level optimization method and the proposed solution. The analysis of results from six simulation cases is

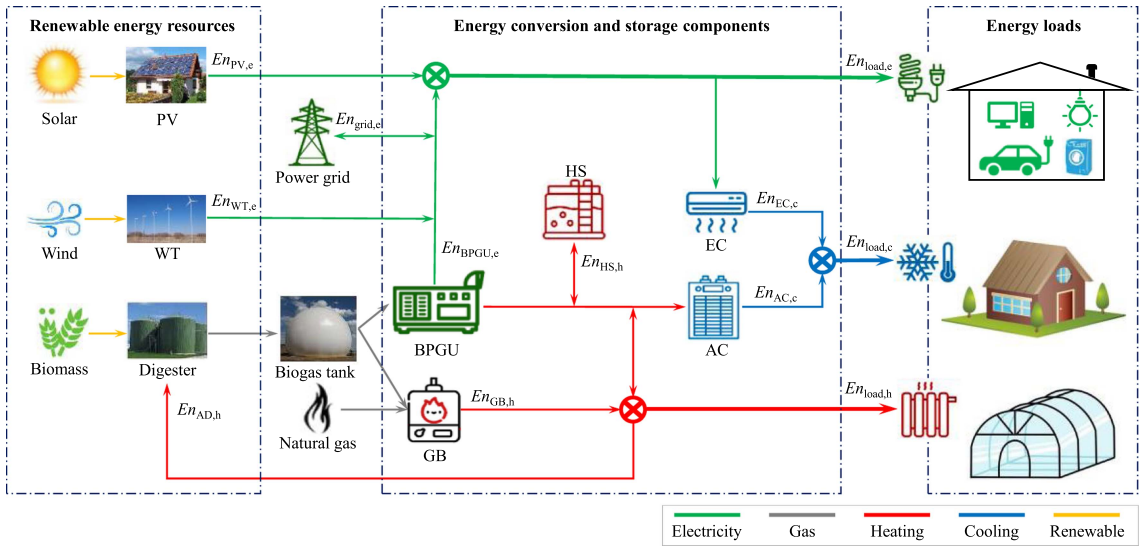

Fig. 1. Schematic of the biogas–solar–wind IES.

detailed in Section IV. Finally, conclusions are summarized in Section V.

II. System Description Based on Exergy Hub Model

A. Structure of IES

The structure of a biogas–solar–wind IES is illustrated in Fig. 1. This IES combines biogas, electricity, heat and cold energy within a specified region. Solar and wind energies are converted into electricity using PV cells and WT, while biomass is transformed into biogas using an AD. To ensure consistent and efficient biogas production, a medium-temperature fermentation process is used and the AD is maintained at 35°C [15]. The amount of heat energy required by the digester fluctuates with the ambient temperature after the capacity of the AD and the fermentation temperature are set owing to heat loss.

The IES includes various energy conversion components: a BPGU, an AC, an EC, and a GB. The BPGU serves as a cogeneration component, converting biogas into electricity and waste heat, with a portion of this waste heat being recycled to sustain the fermentation temperature of the AD. The IES is grid-connected to maintain electricity balance, drawing electricity from the grid when electricity generation is deficient or selling excess electricity back to the grid. Given the limitation on the daily production of biogas, natural gas stands as an auxiliary fuel for the GB, ensuring the provision of heat in case of insufficient biogas. Additionally, a HS unit is installed to enhance the operational flexibility of the system and maximize the usage of recovered waste heat.

B. Biogas Production Model

Within the model, the fermentation temperature is posited as the sole influencing factor of biogas production once the biomass type is selected. The biogas comprises 60% methane (CH_4) [15], and the methane generation rate from the AD is calculated using the formula provided in:

$$\gamma_{\mathrm{CH_4}} = \frac{BS}{HRT}\left(1 - \frac{K}{(0.013T_{\mathrm{AD}} - 0.129)\,HRT - 1 + K}\right) \tag{1}$$

The volume of the AD can be calculated using the required biogas yield in one day:

$$V_{\mathrm{AD}} = \frac{0.6D_{\mathrm{bio}}}{\gamma_{\mathrm{CH_4}}} \tag{2}$$

The thermal energy requirements of the AD include two components: first, for heating the feedstock to initiate digestion and, second, for compensating the thermal energy losses to sustain the set fermentation temperature. The heating balance for the AD can be expressed using the following formula:

$$\rho V_{\mathrm{AD}} SHC_{\mathrm{bf}} \frac{dT_{\mathrm{AD}}}{d\tau} = En_{\mathrm{AD,h}} - \frac{\rho V_{\mathrm{AD}} SHC_{\mathrm{bf}}}{24HRT}\left(T_{\mathrm{AD}} - T_{\mathrm{a}}\right) - En_{\mathrm{AD,loss,h}} \tag{3}$$

where ρ and SHC_{bf} represent the density and specific heat capacity of biomass feedstock, respectively. Their values are assumed to be the same as those of water, and the heat dissipated by the AD is expressed as

$$En_{\mathrm{AD,loss,h}} = UA\left(T_{\mathrm{AD}} - T_{\mathrm{a}}\right) \tag{4}$$

where U represents the overall heat transfer coefficient and is assumed be equal to 0.01 kW/(m^2·°C) and A represents the digester surface area. Herein, a cylindrical digester is employed, and its aspect ratio is 60%.

C. Exergy Analysis

Exergy, as defined by the second law of thermodynamics, accounts for both the quantity and quality of energy and is thus crucial in assessing the comprehensive utilization of energy within IESs [25]. This study employs exergy analysis based on

the EQC to facilitate the efficient use of energy. The EQC describes the relation between energy quantity and quality, which is expressed as

$$\lambda_n = \frac{Ex_n}{En_n} \tag{5}$$

The system exergy efficiency is denoted as

$$\eta_{\text{ex}} = \frac{Ex_{\text{out}}}{Ex_{\text{in}}} \tag{6}$$

The EQC varies based on the type and state of energy and temperature conditions. The EQC for renewable energy (λ_{re}) is assigned a value of zero [25]. EQCs for natural gas and biogas are derived using the following formulas:

$$\lambda_{\text{ng}} = 1 - \frac{T_{\text{a}}}{T_{\text{ng}} - T_{\text{a}}} \ln \frac{T_{\text{ng}}}{T_{\text{a}}} \tag{7}$$

$$\lambda_{\text{bio}} = 1 - \frac{T_{\text{a}}}{T_{\text{bio}} - T_{\text{a}}} \ln \frac{T_{\text{bio}}}{T_{\text{a}}} \tag{8}$$

The EQC of electricity is set to 1, while the EQCs of the hot and cold water are respectively calculated as follows:

$$\lambda_{\text{h}} = 1 - \frac{T_{\text{a}}}{T_{\text{h}}} \tag{9}$$

$$\lambda_{\text{c}} = \frac{T_{\text{a}}}{T_{\text{c}}} - 1 \tag{10}$$

The energy conversion processes in the IES can be described as follows:

$$Ex_{\text{BPGU,e}} = \lambda_{\text{e}} En_{\text{BPGU,e}} = \frac{\lambda_{\text{e}}}{\lambda_{\text{bio}}} Ex_{\text{BPGU,bio}} \eta_{\text{BPGU,e}} \tag{11}$$

$$Ex_{\text{BPGU,h}} = \lambda_{\text{h}} En_{\text{BPGU,h}} = \frac{\lambda_{\text{h}}}{\lambda_{\text{bio}}} Ex_{\text{BPGU,bio}} \eta_{\text{BPGU,h}} \tag{12}$$

$$Ex_{\text{EC,c}} = \lambda_{\text{c}} En_{\text{EC,c}} = \frac{\lambda_{\text{c}}}{\lambda_{\text{e}}} Ex_{\text{EC,e}} \eta_{\text{EC}} \tag{13}$$

$$Ex_{\text{AC,c}} = \lambda_{\text{c}} En_{\text{AC,c}} = \frac{\lambda_{\text{c}}}{\lambda_{\text{h}}} Ex_{\text{AC,h}} \eta_{\text{AC}} \tag{14}$$

$$\begin{aligned} Ex_{\text{GB,h}} &= \lambda_{\text{h}} En_{\text{GB,h}} \\ &= \left(\frac{\lambda_{\text{h}}}{\lambda_{\text{ng}}} Ex_{\text{GB,ng,in}} + \frac{\lambda_{\text{h}}}{\lambda_{\text{bio}}} Ex_{\text{GB,bio,in}} \right) \eta_{\text{GB}} \end{aligned} \tag{15}$$

The aforementioned formulas represent the exergy input/output models of the BPGU, EC, AC, and GB respectively. A greater product of the ratio of two EQCs and the conversion efficiency within any given equation indicates a higher exergy efficiency of the component.

The power generation efficiency of the BPGU is expressed as follows:

$$\begin{aligned} \eta_{\text{BPGU,e}} &= \eta_{\text{BPGU,e}}^{\text{rated}} \left(0.13 + 2.47 \frac{En_{\text{BPGU,e}}}{N_{\text{BPGU}}} - 1.6 \left(\frac{En_{\text{BPGU,e}}}{N_{\text{BPGU}}} \right)^2 \right) \end{aligned} \tag{16}$$

where the rated power generation efficiency of BPGU is determined as follows [7]:

$$\eta_{\text{BPGU,e}}^{\text{rated}} = \left(0.102 \frac{LHV_{\text{bio}}}{LHV_{\text{ng}}} + 0.897 \right) 28.08 (N_{\text{BPGU}})^{0.0563} \tag{17}$$

D. Exergy Hub Model

To analyze the multi-energy conversion and coupling of the IES, a coupling matrix is established based on the traditional energy hub model. This matrix can describe the transmission, conversion, and storage states of different forms of energy within the system, as expressed in (18).

$$\underbrace{\begin{bmatrix} En_{\text{load,e}} \\ En_{\text{load,h}} \\ En_{\text{load,c}} \end{bmatrix}}_{\mathbf{En_{load}}} = \underbrace{\begin{bmatrix} 1 & 1 & 1 & 1 & 0 & 0 & 0 & \frac{-1}{\eta_{\text{EC}}} & 0 \\ 0 & 0 & 0 & \frac{\eta_{\text{BPGU,h}}}{\eta_{\text{BPGU,e}}} & 1 & 1 & -1 & 0 & \frac{-1}{\eta_{\text{AC}}} \\ 0 & 0 & 0 & 0 & 0 & 0 & 0 & 1 & 1 \end{bmatrix}}_{\mathbf{C}} \underbrace{\begin{bmatrix} En_{\text{grid,e}} \\ En_{\text{PV,e}} \\ En_{\text{WT,e}} \\ En_{\text{BPGU,e}} \\ En_{\text{GB,h}} \\ En_{\text{HS,h}} \\ En_{\text{AD,h}} \\ En_{\text{EC,c}} \\ En_{\text{AC,c}} \end{bmatrix}}_{\mathbf{En_{state}}} \tag{18}$$

In (18), η represents the energy conversion efficiency, which reflects only the variations in energy quantity. Therefore, the EQCs are introduced into the coupling matrix to construct an exergy hub model that can simultaneously describe the transformations in energy quantity and quality. The exergy vectors of energy loads and state variables are respectively expressed as follows:

$$\mathbf{Ex_{load}} = \lambda_{\mathbf{load}} \mathbf{En_{load}} \tag{19}$$

$$\mathbf{Ex_{state}} = \lambda_{\mathbf{state}} \mathbf{En_{state}} \tag{20}$$

As the diagonal matrices $\lambda_{\mathbf{load}}$ and $\lambda_{\mathbf{state}}$ are invertible, the relationship between the $\mathbf{Ex_{load}}$ and $\mathbf{Ex_{state}}$ can be calculated as follows:

$$\mathbf{Ex_{load}} = \lambda_{\mathbf{load}} \mathbf{C} \lambda_{\mathbf{state}}^{-1} \mathbf{Ex_{state}} \tag{21}$$

Thus, the exergy hub model of the IES can intuitively represent the exergy coupling constraints between the system states and outputs, which is expressed as follows:

$$\underbrace{\begin{bmatrix} Ex_{\text{load,e}} \\ Ex_{\text{load,h}} \\ Ex_{\text{load,c}} \end{bmatrix}}_{\mathbf{Ex_{load}}} = \underbrace{\begin{bmatrix} 1 & 1 & 1 & 1 & 0 & 0 & 0 & \frac{-1}{\lambda_{\text{c}} \eta_{\text{EC}}} & 0 \\ 0 & 0 & 0 & \frac{\lambda_{\text{h}} \eta_{\text{BPGU,h}}}{\eta_{\text{BPGU,e}}} & 1 & 1 & -1 & 0 & \frac{-\lambda_{\text{h}}}{\lambda_{\text{c}} \eta_{\text{AC}}} \\ 0 & 0 & 0 & 0 & 0 & 0 & 0 & 1 & 1 \end{bmatrix}}_{\mathbf{C'}}$$

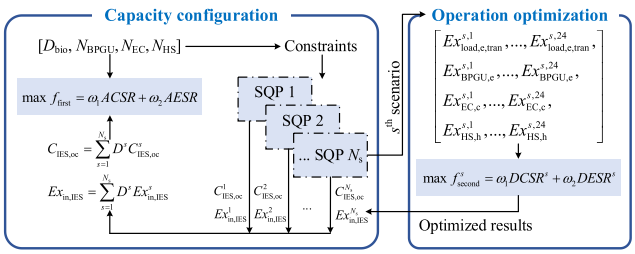

Fig. 2. Schematic of the bi-level optimization framework.

$$\mathbf{Ex_{state}} = \begin{bmatrix} Ex_{\mathrm{grid,e}} \\ Ex_{\mathrm{PV,e}} \\ Ex_{\mathrm{WT,e}} \\ Ex_{\mathrm{BPGU,e}} \\ Ex_{\mathrm{GB,h}} \\ Ex_{\mathrm{HS,h}} \\ Ex_{\mathrm{AD,h}} \\ Ex_{\mathrm{EC,c}} \\ Ex_{\mathrm{AC,c}} \end{bmatrix} \tag{22}$$

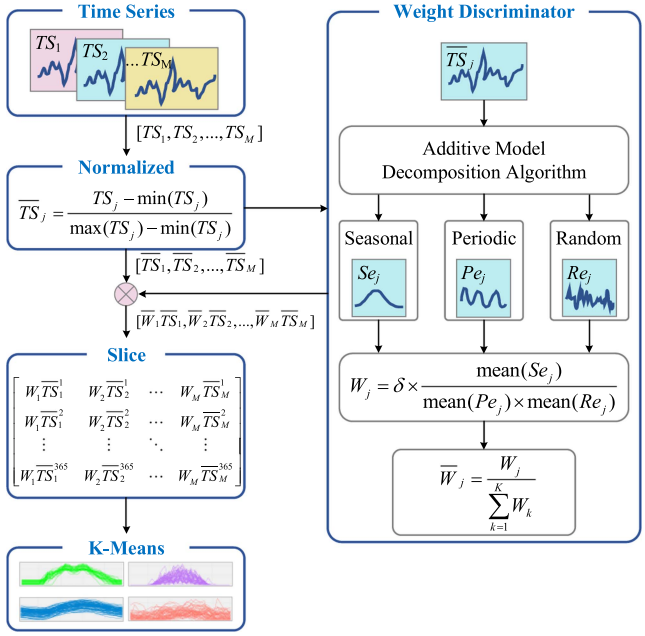

Fig. 3. Flowchart for full-time-series clustering method based on multi-attribute weighting.

III. Bi-level Optimal Design

A. Overall Framework

Unlike conventional design methods that focus only on optimizing energy conversion and storage components, this study incorporates the thermodynamic model-based biogas production optimization and a DR program into the combined capacity and operation optimization. This enables the synergistic optimization of renewables, energy conversion and storage, and demand components within the IES. However, an IES encompasses numerous components with diverse functional attributes that interact restrictively during the optimization process. Given the variation in source–load scenarios and intricate interplay between capacity and operation and nonlinear operational constraints, the optimal design model is considerably complex.

A bi-level optimization method is devised in this study to address the aforementioned complex optimal design problem by employing a nested optimization approach to develop interaction mechanisms between different levels of decision-making. The technical roadmap of the proposed method is depicted in Fig. 2. The first level is the capacity configuration that comprehensively evaluates energy, economy, and environmental performance to optimize the capacities of renewable, energy conversion, and storage components. The outcomes of the first level serve as constraints for the second level. The second level is multi-scenario supply–demand coordinated operation optimization, which optimizes the operation scheme of the energy conversion and storage components, as well as the electricity load curve, using SQP. The goal of the second level is partially derived from the objectives of the first level. This level feeds back the optimized results to the first level for iterative computation. The process culminates in determining the optimal capacity and operation scheme. Furthermore, to enhance the representativeness of the operation scenarios used in the optimization method, this study develops a full-time-series clustering method based on multi-attribute weighting.

B. Full-Time-Series Clustering Method Based on Multi-Attribute Weighting

Considering the inherent periodicity, randomness, and seasonality of renewable energy and loads, this study proposes a full time-series clustering method that incorporates multi-attribute weighting to derive representative source–load scenarios (Fig. 3).

First, the source–load time series data for the entire year are normalized.

$$\overline{TS}_j = \frac{TS_j - \min(TS_j)}{\max(TS_j) - \min(TS_j)} \tag{23}$$

Subsequently, a discriminator is formulated for calculating the weights of different types of data using an additive model decomposition algorithm, which decomposes the j-th full-year time-series data.

$$Se_j, Pe_j, Re_j \leftarrow AdditiveModelDecompositionAlgorithm(\overline{TS}_j) \tag{24}$$

To accurately assess the clustering importance of various renewables and loads, a multi-attribute index calculation formula is developed:

$$W_j = \delta \times \frac{\mathrm{mean}(Se_j)}{\mathrm{mean}(Pe_j) \times \mathrm{mean}(Re_j)} \tag{25}$$

where δ represents a hyperparameter set to avoid excessive differences in the magnitude of the numerator and denominator,

and mean(·) represents a function that solves for the mean. Thereafter, the clustering weights are obtained as follows:

$$\overline{W}_j = \frac{W_j}{\sum_{k=1}^{K} W_k} \tag{26}$$

The obtained clustering weights of different source–load time series data is multiplied by the normalized sequence data to obtain

$$L_j = \overline{W}_j \times \overline{TS}_j \tag{27}$$

Finally, $\mathbf{L} = [L_1, L_2, \ldots L_M] \in \mathbb{R}^{M\times 8760}$ is sliced and then clustered using the conventional K-Means algorithm to obtain typical source–load scenarios.

C. First Level Optimization Model

1) Objective Function: Optimization objective of the first level model is maximizing the annual cost saving ratio (ACSR) and annual exergy saving ratio (AESR), which is described as

$$\max f_{\text{first}} = \omega_1 ACSR + \omega_2 AESR \tag{28}$$

$$ACSR = \frac{C_{\text{SP}} - C_{\text{IES}}}{C_{\text{SP}}} \times 100\% \tag{29}$$

$$AESR = \frac{Ex_{\text{in,SP}} - Ex_{\text{in,IES}}}{Ex_{\text{in,SP}}} \times 100\% \tag{30}$$

where $\omega_1 + \omega_2 = 1$. The reference system is a SP system, where electricity is supplied by the power grid and the heating and cooling loads are fulfilled by a GB and an EC, respectively [13]. The annual total cost of the IES incurs the annualized investment, operation, and maintenance costs. The annualized investment cost is denoted as follows:

$$C_{\text{IES,ic}} = \sum_{i\in\Omega} N_i UIC_i R_i \tag{31}$$

$$R_i = \frac{r(1+r)^{n_i}}{(1+r)^{n_i} - 1} \tag{32}$$

where r denotes the interest rate and is set to 6%.

The maintenance cost can be expressed as follows:

$$C_{\text{IES,mc}} = \sum_{i\in\Omega} N_i UMC_i \tag{33}$$

The annual operation cost comprises biomass feedstock ($C_{\text{IES,bf}}$), natural gas ($C_{\text{IES,ng}}$), electricity purchasing or selling ($C_{\text{IES,grid}}$), and carbon emission costs, expressed as follows:

$$\begin{aligned} C_{\text{IES,oc}} &= \sum_{s=1}^{N_s} D^s C^s_{\text{IES,oc}} \\ &= \sum_{s=1}^{N_s} D^s \left(C^s_{\text{IES,bf}} + C^s_{\text{IES,ng}} + C^s_{\text{IES,grid}} + P_{\text{ct}} CE^s_{\text{IES}}\right) \end{aligned} \tag{34}$$

$$Ex_{\text{in,IES}} = \sum_{s=1}^{N_s} D^s Ex^s_{\text{in,IES}} \tag{35}$$

$$\sum_{s=1}^{N_s} D^s = 365 \tag{36}$$

The annual total cost and exergy consumption of the SP system are evaluated similar to those of the IES.

2) Optimization Variables: The optimization variables of the first level model include the average daily biogas yield and the rated capacities of the BPGU, EC, and HS units, expressed as follows:

$$X_{\text{first}} = [D_{\text{bio}}, N_{\text{BPGU}}, N_{\text{EC}}, N_{\text{HS}}] \tag{37}$$

The capacities of PV and WT can be determined based on the installation conditions, and the capacity of the AD can be calculated by D_{bio} using (2).

3) Constraints: To ensure the rationality of the configuration, the first level optimization model should satisfy the following constraints:

$$0 \le D_{\text{bio}} \le D_{\text{bio,max}} \tag{38}$$

$$0 \le N_i \le N_{i,\text{max}}, i \in [\text{BPGU}, \text{EC}, \text{HS}] \tag{39}$$

D. Second Level Optimization Model

1) Objective Function: The second level comprises N_s optimization subproblems due to the independence of the IES operation scenarios. The aim of this level aligns with that of the first level, i.e., to minimize the daily exergy consumption and operation costs of the IES under the constraints of the optimization outcomes from the first level. Consequently, the objective function for each subproblem is expressed as follows:

$$\max f^s_{\text{second}} = \omega_1 DCSR^s + \omega_2 DESR^s \tag{40}$$

$$DCSR^s = \frac{C^s_{\text{SP,oc}} - C^s_{\text{IES,oc}}}{C^s_{\text{SP,oc}}} \times 100\% \tag{41}$$

$$DESR^s = \frac{Ex^s_{\text{in,SP}} - Ex^s_{\text{in,IES}}}{Ex^s_{\text{in,SP}}} \times 100\% \tag{42}$$

$$\begin{aligned} C^s_{\text{IES,oc}} = {} & \alpha^s_{\text{ng}} \left(\frac{P_{\text{ng}}}{LHV_{\text{ng}}} + P_{\text{ct}}\mu_{\text{ng}}\right) En^s_{\text{ng}} + C^s_{\text{IES,bf}} \\ & + P_{\text{ct}}\mu_{\text{bio}} En^s_{\text{bio}} \\ & + \sum_{t=1}^{24} \left(P^{s,t}_{\text{grid}} En^{s,t}_{\text{grid,e}} + P_{\text{ct}}\mu_{\text{grid}} En^{s,t}_{\text{grid,e,+}}\right) \end{aligned} \tag{43}$$

$$En^s_{\text{ng}} = \sum_{t=1}^{24} (En^{s,t}_{\text{BPGU,bio}} + En^{s,t}_{\text{GB,in}})\Delta t - D_{\text{bio}} LHV_{\text{bio}} \tag{44}$$

$$\alpha^s_{\text{ng}} = \begin{cases} 1, En^s_{\text{ng}} \ge 0 \\ 0, En^s_{\text{ng}} < 0 \end{cases} \tag{45}$$

$$En^s_{\text{bio}} = \begin{cases} D_{\text{bio}} LHV_{\text{bio}}, En^s_{\text{ng}} \ge 0 \\ \sum_{t=1}^{24} (En^{s,t}_{\text{BPGU,bio}} + En^{s,t}_{\text{GB,in}})\Delta t, En^s_{\text{ng}} < 0 \end{cases} \tag{46}$$

$$Ex^{s}_{\text{in,IES}} = \sum_{t=1}^{24} (Ex^{s,t}_{\text{re}} + Ex^{s,t}_{\text{grid,e,+}} + Ex^{s,t}_{\text{ng}})\Delta t \tag{47}$$

where $\alpha_{\text{ng,d}}$ is equal to 1, indicating that natural gas is used to drive the GB.

2) Optimization Variables: The optimization variables include the hourly translational electricity load and hourly operation plans of the BPGU, EC, and HS, as follows:

$$X^{s}_{\text{second}} = \begin{bmatrix} Ex^{s,1}_{\text{load,e,tran}}, \ldots, Ex^{s,24}_{\text{load,e,tran}}, \\ Ex^{s,1}_{\text{BPGU,e}}, \ldots, Ex^{s,24}_{\text{BPGU,e}}, \\ Ex^{s,1}_{\text{EC,c}}, \ldots, Ex^{s,24}_{\text{EC,c}}, \\ Ex^{s,1}_{\text{HS,h}}, \ldots, Ex^{s,24}_{\text{HS,h}} \end{bmatrix} \tag{48}$$

3) Constraints: The objective function is subject to the supply–demand coordinated operation constraints, including energy conversion constraints in (11)–(15), exergy balance constraints in (22), energy storage and DR constraints. The HS is constrained by the following formulas.

$$Ex^{s,t+1}_{\text{HS,h,state}} = \eta_{\text{HS}} Ex^{s,t}_{\text{HS,h,state}} + Ex^{s,t}_{\text{HS,h}}, \ \forall s,t \tag{49}$$

$$Ex^{s,0}_{\text{HS,h,state}} = Ex^{s,24}_{\text{HS,h,state}}, \ \forall s,t \tag{50}$$

$$0 \le En^{s,t}_{\text{HS,h,state}} \le N_{\text{HS}}, \ \forall s,t \tag{51}$$

This study introduces an electrical DR model. Shedding electricity load is not discussed to avoid insufficiency of the component capacity. The total electricity load in an operation cycle after considering the DR remains unchanged. Thus, the DR model is expressed as follows [26]:

$$Ex^{s,t}_{\text{load,e}} = Ex^{s,t}_{\text{load,e,ori}} + Ex^{s,t}_{\text{load,e,tran}}, \ \forall s,t \tag{52}$$

$$-\beta Ex^{s,t}_{\text{load,e,ori}} \le Ex^{s,t}_{\text{load,e,tran}} \le \beta Ex^{s,t}_{\text{load,e,ori}}, \ \forall s,t \tag{53}$$

$$\sum_{t=1}^{24} Ex^{s,t}_{\text{load,e,tran}} \Delta t = 0, \ \forall s,t \tag{54}$$

Additionally, the fuel usage of the BPGU within a scenario must not surpass the mean daily biogas production. The biogas storage tank is responsible for ensuring a consistent daily supply of biogas. Moreover, the outputs of the BPGU and EC are constrained to their rated capacities generated from the first level.

$$\sum_{t=1}^{24} En^{s,t}_{\text{BPGU,bio}} \Delta t \le D_{\text{bio}} LHV_{\text{bio}}, \ \forall s \tag{55}$$

$$0 \le En^{s,t}_{\text{BPGU,e}} \le N_{\text{BPGU}}, \ \forall s,t \tag{56}$$

$$0 \le En^{s,t}_{\text{EC,c}} \le N_{\text{EC}}, \ \forall s,t \tag{57}$$

E. Solving Method

The proposed bi-level optimization model is a mixed-integer nonlinear programming problem that contains numerous integers, continuous decision variables, and nonlinear constraints. Thus, a sparse nonlinear optimizer is embedded into a GA to handle the complex optimization problem. The solving method is illustrated in Fig. 4. In this method, the GA computes individual fitness by repeatedly employing the SQP to minimize the operation cost and exergy consumption of each individual. In the second level, constraints from the first level capacity results are received for performing the optimization of the operation scheme. The optimized findings are cycled back to the first level for iterative calculations until the optimal IES design solution is obtained.

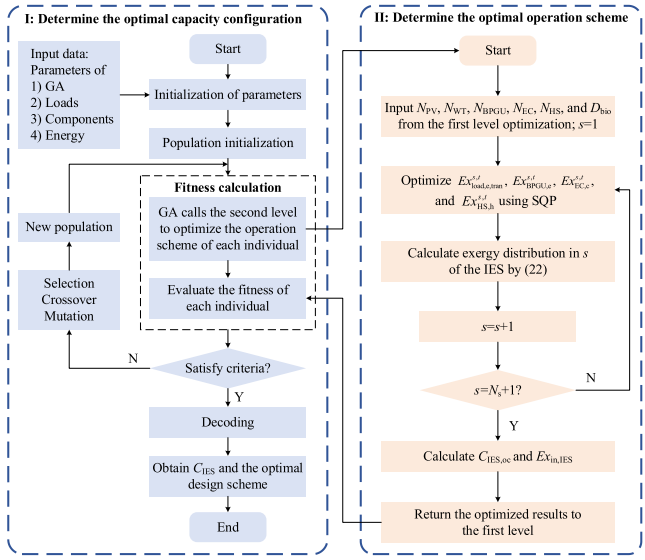

Fig. 4. Flowchart of solving method.

TABLE I
NUMBERS OF DAYS FOR REPRESENTATIVE SCENARIOS

Scenario	Number of days	Scenario	Number of days
1	46	5	43
2	39	6	63
3	46	7	42
4	30	8	56

IV. CASE STUDIES

A. System Parameters

The IES outlined in Fig. 1 is employed as a test system. For case studies, typical rural loads and weather data from northern China are used. Using the clustering method presented in Section III, representative source–load scenarios (with PV and WT rated capacities of 50 kW each) are obtained, as depicted in Fig. 5. These scenarios are categorized into heating (1, 3, 7), cooling (2, 4, 8), and transition scenarios (5, 6), with the respective number of days detailed in Table I. The primary economic and efficiency parameters of the system components are outlined in Table II [27], [28], whereas the time-of-use electricity tariffs are summarized in Table III [27]. The emission conversion factor of the grid is 0.968 kg/kWh [9], and the technical parameters of natural gas and biogas are compiled in Table IV [9]. The carbon tax is set at 0.3 CNY/kg [29], and the investment cost for an AD with gas purification and storage capabilities are posited at 3000 CNY/m^3 [6]. Biomass feedstock is priced at 250 CNY/t [30]. The GA operates over 200 generations with a population size of 100.

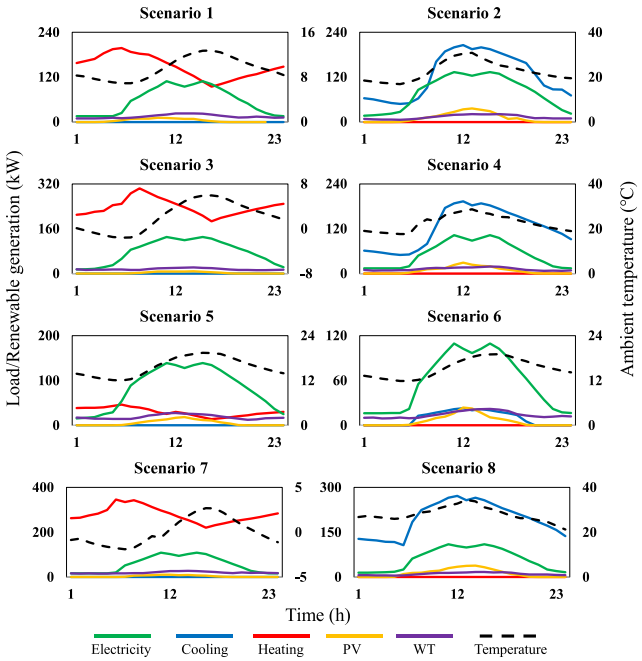

Fig. 5. Representative source–load scenarios.

TABLE II
MAIN PARAMETERS OF COMPONENTS

Component	Capital cost	Maintenance cost	Efficiency	Lifetime
PV	3000 CNY/kW	40 CNY/kW	–	25 years
WT	3500 CNY/kW	37 CNY/kW	–	20 years
BPGU	2000 CNY/kW	45 CNY/kW	–	20 years
AC	1200 CNY/kW	30 CNY/kW	0.9	20 years
GB	330 CNY/kW	38 CNY/kW	0.9	20 years
EC	1200 CNY/kW	35 CNY/kW	3.0	20 years
HS	90 CNY/kWh	5 CNY/kWh	0.9	20 years

TABLE III
TIME-OF-USE ELECTRICITY PRICES

Electricity prices	10:00–13:00; 18:00–23:00	7:00–10:00; 13:00–18:00	23:00–7:00
Purchasing (CNY/kWh)	0.925	0.614	0.402
Selling (CNY/kWh)	0.4	0.3	0.2

TABLE IV
TECHNICAL PARAMETERS OF NATURAL GAS AND BIOGAS

Gas	Lower heat value (kWh/Nm^3)	Price (CNY/Nm^3)	Emission conversion factor (kg/kWh)
Natural gas	9.3	2.9	0.22
Biogas	6.11	–	0.05

To verify the feasibility and efficiency of the proposed bi-level optimal design method, six cases are executed:

Case 1: The design scheme of the biogas–solar–wind IES is determined using the bi-level optimization with the objectives of economy and exergy efficiency ($\omega_1 = \omega_2 = 1/2$).

Case 2: The design scheme of the biogas–solar–wind IES is determined using the bi-level optimization with the objectives of economy and energy efficiency ($\omega_1 = \omega_2 = 1/2$).

TABLE V
CAPACITY RESULTS OF IESS IN SIX CASES

Case	Daily biogas production (Nm^3/d)	BPGU (kW)	AC (kW)	EC (kW)	GB (kW)	HS (kWh)
1	1240	125	222	50	429	30
2	720	110	113	200	355	40
3	640	80	112	160	362	20
4	480	60	79	198	412	90
5	-	80	132	140	289	50
6	620	110	132	140	418	75

TABLE VI
DIFFERENCES IN COST AMONG CACES

Case	$C_{\text{IES,ic}}$ & $C_{\text{IES,mc}}$ ($\times 10^4$ CNY)	$C_{\text{IES,oc}}$ ($\times 10^4$ CNY)	C_{IES} ($\times 10^4$ CNY)	ACSR	Pb_{IES} (years)
1	36.35	54.11	90.46	18.50%	6.5
2	26.17	57.19	83.36	24.89%	4.5
3	23.44	54.26	77.70	30.01%	3.7
4	20.58	65.89	86.47	22.09%	4.5
5	10.70	69.01	79.71	28.19%	5.6
6	24.18	55.27	79.45	28.42%	3.9

Case 3: The design scheme of the biogas–solar–wind IES is determined using the bi-level optimization with the economy objective.

Case 4: The design scheme of the biogas–solar–wind IES is determined using a single-level optimization with the economy objective, not considering operation optimization.

Case 5: The design scheme of the natural gas–solar–wind IES is determined using the bi-level optimization with the economy objective.

Case 6: The design scheme of the biogas–solar–wind IES is determined using the bi-level optimization with the economy objective, not considering electrical DR.

A comparative assessment of cases 1, 2, and 3 is conducted to understand the influence of incorporating energy quality variation within the IES design. Further comparison between cases 3, 4, 5, and 6 indicates the contributions of the combined capacity and operation optimization and synergy of renewables, energy conversion, storage, and demand to optimal design schemes. Furthermore, the payback period is applied as an indication to evaluate the return of investment for IESs [31], which can help businesses decide whether or not to invest in an IES. The payback period of the IES can be expressed as follows:

$$Pb_{\text{IES}} = \frac{C_{\text{IES,cap}} - C_{\text{SP,cap}}}{C_{\text{SP,oc}} - C_{\text{IES,oc}}} \tag{58}$$

B. Results and Analysis

1) Comparative Analysis of Design Results: Table V summarizes the optimized capacity configurations of IESs in the six cases. Table VI presents the annual total cost, annualized investment, maintenance, and operation costs, and ACSR of each case. Irrespective of considering exergy efficiency or energy efficiency, incorporating multiple objectives into the optimal design of the IES tends to diminish its economic performance. The AESRs for cases 1, 2, and 3 are 79.21%, 55.97%, and 56.62%, respectively. Given the BPGU is an electricity and

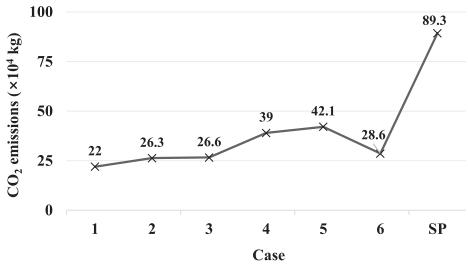

Fig. 6. Annual carbon emissions of six cases and SP system.

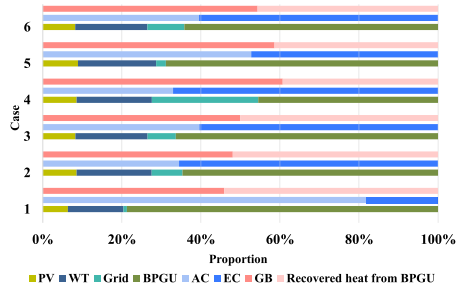

Fig. 7. Proportion of energy supplied by each component in six cases.

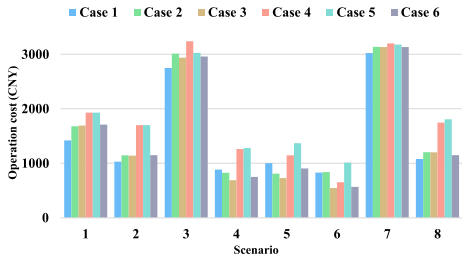

Fig. 8. Operation cost of each scenario in six cases.

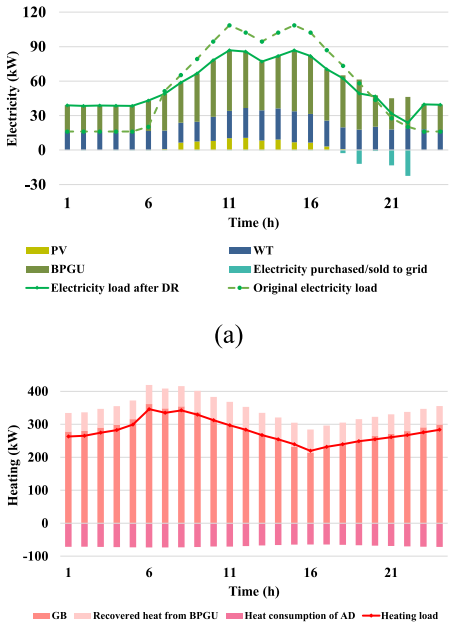

Fig. 9. Daily operation scheme of scenario 7 in case 3: electricity balance (a), heating balance (b).

heat coupling component with high exergy efficiency, case 1 exhibits the largest daily biogas production and rated capacity of BPGU, along with high investment cost. A comparison between cases 1 and 2 reveals a larger AC capacity in case 1, whereas the EC capacity is larger in case 2, attributable to the superior exergy efficiency of AC and the higher energy efficiency of EC, respectively. Case 4, which employs the following electricity load operation strategy, necessitates the largest HS capacity to fulfill passive energy storage functions.

The economic aspect of IES improves with the introduction of synergy optimization. The rated capacities of BPGU, AC, GB, and HS notably increase when the design method omits DR. This indicated that the DR facilitates peak shaving and valley filling, leading to a more reasonable capacity configuration. As demonstrated by cases 3 and 5, establishing a biogas fermentation system augments the investment costs; however, the savings on operation costs are more pronounced. In comparison with the single-level optimization method, the bi-level optimal design method presented herein furnishes more effective solutions. When only economy is the optimization objective, case 3 has the shortest payback period from the return of the investment viewpoint while case 5 has the longest payback period due to not installing a biogas system. In addition, adopting a fixed operation strategy will increase the payback period of the system design solution.

Fig. 6 shows that the annual carbon emissions of the six IES cases and a SP system. The application of the IES solutions can substantially reduce carbon emissions than the SP system. Moreover, the biogas-based IESs are advantageous in terms of carbon emission reduction than the natural gas-based IES. A comparison of cases 1, 2, and 3 reveals that the consideration of exergy objective has promoting effect on reducing carbon emissions. A comparison of cases 3, 4, and 6 suggests that incorporating the advanced operation technology and synergy optimization into the system optimal design can further reduce carbon emissions.

2) Comparative Analysis of Operation Schemes: The proposed bi-level optimization method is assessed by comparing the annual energy contribution of each component across the six scenarios. In Fig. 7, the horizontal axis represents the total energy consumption of IES. The electricity consumption includes building electricity loads, electricity usage by EC, and sold electricity. Heat consumption refers to the heating demands of the buildings, AC and AD, while cooling consumption relates to the cooling requirements of the buildings. The HS unit, not contributing to energy production or conversion, is omitted from this analysis.

According to Fig. 7, case 1 exhibits the highest proportions of electricity and cold energy supplied by BPGU and AC, respectively, owing to the exergy objective consideration, setting it distinctly apart from case 2. Case 4 without operation optimization exhibits the lowest BPGU energy contribution; thus, the biogas demand is also the lowest, which explains the reason for its

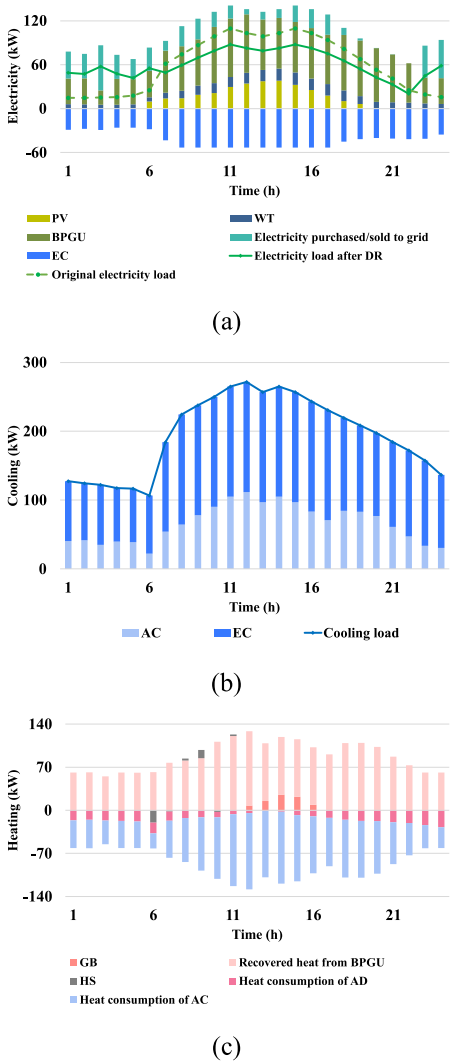

Fig. 10. Daily operation scheme of scenario 8 in case 3: (a) electricity balance, (b) cooling balance, and (c) heating balance.

lowest daily biogas yield value (Table V). Given the higher lower heat value of natural gas compared with biogas, the energy contribution from BPGU in the natural gas-based IES exceeds that of case 3. However, case 3 outperforms case 5 in terms of operation costs, indicating that the average generation cost for natural gas-based IES is higher than for biogas-based IES. The findings from case 6 illustrate that omitting DR results in a considerable increase in grid reliance, leading to high operation costs.

Fig. 8 compares the operation costs for each scenario for the six cases. In all cases, the transition scenarios exhibit relatively low operation costs compared with cooling and heating scenarios. Moreover, for the biogas-based IESs, cooling scenarios consistently demonstrate lower operation costs than heating scenarios that encounter higher fermentation heating demands. A comparative analysis between case 3 and cases 4, 5, and 6 highlights the economic benefits of case 3 in each source–load scenario, further demonstrating the cost-saving advantages of synergy optimization.

3) Result Analysis of Operation Schemes: The operation scheme results for the biogas–solar–wind IES under case 3 are illustrated in Figs. 9 and 10, which depict scenarios 7 and 8, respectively. Note that parameters such as sold electricity, electrical input for the EC, heat consumption for AC and AD, along with the heat stored in the HS unit, are illustrated beneath the horizontal axis in these figures. The energy flows maintain equilibrium at every instance within the two scenarios, and solid-green curves indicate the optimized electricity loads after DR implementation. The synergy optimization results in a smoother load profile, effectively reducing peak demand and increasing the valley load, thereby optimizing the electricity expenditure and encouraging the active participation of IES components throughout the operation cycle.

As seen in Fig. 9, renewable sources predominantly satisfy the electricity load in a heating scenario. The electricity load response reduces the peak-to-valley discrepancy, ensuring an economically feasible match for the heating demand. In the heating scenario, the low ambient temperature necessitates substantial heat generation to sustain the fermentation temperature. The waste heat recovery alone is insufficient to meet this demand; hence, GB is required to operate extensively. With no surplus heat necessitating storage, the HS unit remains inactive.

In the cooling scenario illustrated in Fig. 10, the electric energy distribution follows a similar pattern to that in the heating scenario, with renewable generation fulfilling the primary energy demand supplemented by the grid. At night, the BPGU activates, recovering a large amount of waste heat. This recovered heat powers the AC to satisfy the cooling demand and is directed to the AD for stable biogas production. Thereafter, any excess heat is stored in the HS. Owing to the high electricity and cooling requirements, coupled with limited biogas availability, the EC operates continuously, and any electrical deficit is compensated by purchasing electricity. Concurrently, the GB is engaged to satisfy the heating deficit.

V. Conclusion

This study proposes a bi-level optimal design method for a biogas–solar–wind IES, aimed at maximizing economic and energetic performance of the system. The proposed method realizes synergistic optimization of renewables, energy conversion, storage, and demand. By addressing the imbalance between the renewable energy production and consumption, the bi-level optimal design method considerably enhances the efficient use of renewable energy sources, resulting in the decreased annual total cost, grid reliance, and exergy consumption. Considering energy quality in the optimization objective, the system design scheme prioritizes the selection of components with high exergy efficiency, such as BPGU and AC, while increasing the biogas consumption. The ACSR of the IES, optimized using the proposed bi-level optimization method, exhibits an increase of 1.59% and 7.92% compared with the cases where synergy optimization is lacking and the single-level design method is used, respectively. Furthermore, it is indicated that the average generation cost for biogas-based IES is substantially lower than that for natural gas-based IES considering the life cycle investment cost. The outcomes of the proposed method can offer valuable insights for the economic and sustainable advancement of renewable energy sources.

REFERENCES

[1] X. Wei, X. Zhang, Y. Sun, and J. Qiu, "Carbon emission flow oriented tri-level planning of integrated electricity-hydrogen-gas system with hydrogen vehicles," *IEEE Trans. Ind. Appl.*, vol. 58, no. 2, pp. 2607–2618, Jul. 2021.

[2] Z. Zhang, C. Wang, H. Lv, F. Liu, H. Sheng, and M. Yang, "Day-ahead optimal dispatch for integrated energy system considering power-to-gas and dynamic pipeline networks," *IEEE Trans. Ind. Appl.*, vol. 57, no. 4, pp. 3317–3328, Apr. 2021.

[3] T. Kunatsa and X. Xia, "Co-digestion of water hyacinth, municipal solid waste and cow dung: A methane optimised biogas-liquid petroleum gas hybrid system," *Appl. Energy*, vol. 304, Dec. 2021, Art. no. 117716.

[4] M. A. Azizi and J. Brouwer, "Progress in solid oxide fuel cell-gas turbine hybrid power systems: System design and analysis, transient operation, controls and optimization," *Appl. Energy*, vol. 215, pp. 237–289, Apr. 2018.

[5] X. Li, L. Zhang, R. Wang, B. Sun, and W. Xie, "Two-stage robust optimization model for capacity configuration of biogas-solar-wind integrated energy system," *IEEE Trans. Ind. Appl.*, vol. 59, no. 1, pp. 662–675, Oct. 2022.

[6] A. Kasaeian, P. Rahdan, M. A. V. Rad, and W.-M. Yan, "Optimal design and technical analysis of a grid-connected hybrid photovoltaic/diesel/biogas under different economic conditions: A case study," *Energy Convers. Manage.*, vol. 198, Oct. 2019, Art. no. 111810.

[7] J. Wang and Y. Yang, "Energy, exergy and environmental analysis of a hybrid combined cooling heating and power system utilizing biomass and solar energy," *Energy Convers. Manage.*, vol. 124, pp. 566–577, Sep. 2016.

[8] W. Gazda and W. Stanek, "Energy and environmental assessment of integrated biogas trigeneration and photovoltaic plant as more sustainable industrial system," *Appl. Energy*, vol. 169, pp. 138–149, May 2016.

[9] T. Wu, S. Bu, X. Wei, G. Wang, and B. Zhou, "Multitasking multi-objective operation optimization of integrated energy system considering biogas-Solar-wind renewables," *Energy Convers. Manage.*, vol. 229, Feb. 2021, Art. no. 113736.

[10] B. Zhou et al., "Optimal scheduling of biogas-solar-wind renewable portfolio for multicarrier energy supplies," *IEEE Trans. Power Syst.*, vol. 33, no. 6, pp. 6229–6239, May 2018.

[11] Y. Wang et al., "Planning and operation method of the regional integrated energy system considering economy and environment," *Energy*, vol. 171, pp. 731–750, Mar. 2019.

[12] C. M. I. Hussain, B. Norton, and A. Duffy, "Technological assessment of different solar-biomass systems for hybrid power generation in Europe," *Renewable Sustain. Energy Rev.*, vol. 68, pp. 1115–1129, Feb. 2017.

[13] J. Wang, F. Dong, Z. Ma, H. Chen, and R. Yan, "Multi-objective optimization with thermodynamic analysis of an integrated energy system based on biomass and solar energies," *J. Cleaner Prod.*, vol. 324, Nov. 2021, Art. no. 129257.

[14] M. B. Eteiba, S. Barakat, M. M. Samy, and W. I. Wahba, "Optimization of an off-grid PV/biomass hybrid system with different battery technologies," *Sustain. Cities Soc.*, vol. 40, pp. 713–727, Jul. 2018.

[15] B. Su, W. Han, X. Zhang, Y. Chen, Z. Wang, and H. Jin, "Assessment of a combined cooling, heating and power system by synthetic use of biogas and solar energy," *Appl. Energy*, vol. 229, pp. 922–935, Nov. 2018.

[16] W. Xu, D. Zhou, X. Huang, B. Lou, and D. Liu, "Optimal allocation of power supply systems in industrial parks considering multi-energy complementarity and demand response," *Appl. Energy*, vol. 275, Oct. 2020, Art. no. 115407.

[17] Y. Fu, H. Lin, B. Feng, C. Ma, Q. Sun, and R. Wennersten, "Off-design characteristics of energy conversion equipment in integrated energy systems," *J. Cleaner Prod.*, vol. 407, Jun. 2023, Art. no. 136941.

[18] L. Ji, X. Liang, Y. Xie, G. Huang, and B. Wang, "Optimal design and sensitivity analysis of the stand-alone hybrid energy system with PV and biomass-CHP for remote villages," *Energy*, vol. 225, Jun. 2021, Art. no. 120323.

[19] L. Zhang, L. Zhang, B. Sun, C. Zhang, and F. Li, "Nested optimization design for combined cooling, heating, and power system coupled with solar and biomass energy," *Int. J. Elect. Power Energy Syst.*, vol. 123, Dec. 2020, Art. no. 106236.

[20] C. Li et al., "Optimal planning of Islanded integrated energy system with solar-biogas energy supply," *IEEE Trans. Sustain. Energy*, vol. 11, no. 4, pp. 2437–2448, Dec. 2019.

[21] Z. Zhang, Y. Huang, Z. Chen, and W.-J. Lee, "Integrated demand response for microgrids with incentive compatible bidding mechanism," *IEEE Trans. Ind. Appl.*, vol. 59, no. 1, pp. 118–127, Sep. 2022.

[22] N. Zhao, W. Gu, Z. Zheng, and T. Ma, "Multi-objective Bi-level planning of the integrated energy system considering uncertain user loads and carbon emission during the equipment manufacturing process," *Renewable Energy*, vol. 216, Nov. 2023, Art. no. 119070.

[23] L. Zhang, B. Sun, and F. Li, "Bi-level optimal design of integrated energy system with synergy of renewables, conversion, storage and demand," in *Proc. IEEE 4th Int. Conf. Smart Power Internet Energy Syst.*, Beijing, China, 2022, pp. 1613–1618.

[24] C. Pan, H. Fan, R. Zhang, J. Sun, Y. Wang, and Y. Sun, "An improved multi-timescale coordinated control strategy for an integrated energy system with a hybrid energy storage system," *Appl. Energy*, vol. 343, Aug. 2023, Art. no. 121137.

[25] X. Hu et al., "Multi-objective planning for integrated energy systems considering both exergy efficiency and economy," *Energy*, vol. 197, Apr. 2020, Art. no. 117155.

[26] Y. Li, B. Wang, Z. Yang, J. Li, and G. Li, "Optimal scheduling of integrated demand response-enabled community-integrated energy systems in uncertain environments," *IEEE Trans. Ind. Appl.*, vol. 58, no. 2, pp. 2640–2651, Mar./Apr. 2022.

[27] Y. Xiang, H. Cai, C. Gu, and X. Shen, "Cost–Benefit analysis of integrated energy system planning considering demand response," *Energy*, vol. 192, Feb. 2020, Art. no. 116632.

[28] W. Huang, N. Zhang, J. Yang, Y. Wang, and C. Kang, "Optimal configuration planning of multi-energy systems considering distributed renewable energy," *IEEE Trans. Smart Grid*, vol. 10, no. 2, pp. 1452–1464, Oct. 2017.

[29] L. Kang et al., "Effects of load following operational strategy on CCHP system with an auxiliary ground source heat pump considering carbon tax and electricity feed in tariff," *Appl. Energy*, vol. 194, pp. 454–466, May 2017.

[30] N. Wu et al., "Analysis of Biomass Polygeneration Integrated energy System based on a mixed-integer nonlinear programming optimization method," *J. Cleaner Prod.*, vol. 271, Oct. 2020, Art. no. 122761.

[31] P. Mago and A. Huedded, "Evaluation of a turbine driven CCHP system for large office buildings under different operating strategies," *Energy Buildings*, vol. 42, pp. 1628–1636, Apr. 2010.